Gating-dependent Mechanism of 4-Aminopyridine Block in Two Related Potassium Channels

G. E. KIRSCH,*‡ and J. A. DREWE‡

From the Departments of *Anesthesiology, and ‡Molecular Physiology and Biophysics, Baylor College of Medicine, Houston, Texas 77030

ABSTRACT 4-aminopyridine (4AP) is widely used as a selective blocker of voltage-activated K^+ currents in excitable membranes, but its mechanism and site of action at the molecular level are not well understood. To address this problem we have analyzed 4AP block in Kv2.1 and Kv3.1, mammalian representatives of the *Drosophila Shab* and *Shaw* subfamilies of voltage-gated K^+ channels, respectively. The two channels were expressed in *Xenopus* oocytes and analyzed at both the macroscopic and single channel levels. Whole cell analysis showed that 4AP sensitivity of Kv3.1 was ~150 times greater than that of Kv2.1. Patch clamp analysis revealed that the mechanism of 4AP block in both channels was qualitatively similar. 4AP reached its blocking site via the cytoplasmic side of the channels, the ON rate for block was strongly accelerated when channels opened and the drug was trapped in closed channels. Single channel analysis showed that 4AP decreased burst duration and increased the latency-to-first-opening. These effects were found to be related, respectively to drug ON and OFF rates in the activated channel. Kv3.1's high 4AP sensitivity relative to Kv2.1 was associated with both a slower OFF rate and therefore increased stability of the blocked state, as well as a faster ON rate and therefore increased access to the binding site. Our results indicate that in both channels 4AP enters the intracellular mouth to bind to a site that is guarded by the gating mechanism. Differences in channel gating as well as differences in the structure of the intracellular mouth may be important for specifying the 4AP sensitivity in related voltage-gated K^+ channels.

INTRODUCTION

4-Aminopyridine (4AP) and tetraethylammonium (TEA) are widely used blockers of voltage-gated K^+ channels that act by different mechanisms and possibly at different sites in the channel. Whereas TEA acts like an open channel blocker that can be displaced by permeant ions and by the closing of the activation gate (Armstrong, 1971; Kirsch, Taglialatela, and Brown, 1991), 4AP's mechanism is complicated by variable interactions with closed, open and inactivated states of the channel (Yeh, Oxford, Wu, and Narahashi, 1976; Ulbricht and Wagner, 1976; Thompson, 1982).

Address correspondence to Dr. Kirsch, One Baylor Plaza, Suite 443A, Houston, Texas 77030.

J. GEN. PHYSIOL. © The Rockefeller University Press · 0022-1295/93/11/0797/20 $2.00
Volume 102 November 1993 797–816

Thus, TEA and its derivatives have been used successfully to probe the ion conduction pathway (Armstrong, 1971; Hartmann, Kirsch, Drewe, Taglialatela, Joho, and Brown, 1991; Yellen, Jurman, Abramson, and MacKinnon, 1991) but 4AP's utility as a probe has not been established because its mechanism and site of action are not well understood.

The main issue is whether 4AP interacts primarily with open or closed channels. Early work on delayed rectifier K^+ currents in axons (Yeh et al., 1976, Ulbricht and Wagner, 1976) focused on 4AP's slow entry into closed channels and relatively rapid exit from open channels, leading to the suggestion that 4AP and TEA mechanisms were reciprocal in the sense that 4AP blocks closed channels whereas TEA blocks open channels. More recent work, also at the macroscopic level, has emphasized the fact that 4AP equilibrates much more rapidly with open than with closed channels, and therefore may be considered to have some of the characteristics of slow open channel blockers such as the long-chain TEA derivatives (Armstrong, 1971; Kirsch et al., 1991). In addition, 4AP appears to compete with inactivation (Thompson, 1982) which itself is coupled to the open state. These results, together with evidence that the rate of 4AP block from the cytoplasmic surface of the channel is slowed by the presence of extracellular permeant ions (Kirsch, Yeh, and Oxford, 1986) suggests that 4AP may provide a useful probe of the cytoplasmic end of the open channel. Differential sensitivity of 4AP to gating conformations suggests that this drug may also serve to probe structures that couple gating to ion conduction.

Despite intensive study at the macroscopic level, little attention has been devoted to 4AP block in single channels, in part because of problems associated with recording K^+ channels in their native environment, including: (*a*) The coupling between 4AP block and channel gating. Many of the apparent discrepancies between different tissues may arise from heterogeneities in gating of mixed populations of different K^+ channels; (*b*) the almost unavoidable presence of multiple voltage-gated K^+ channels of one or more types in native membrane patches which reduces the amount of information that can be extracted from kinetic analysis; and (*c*) The time course of 4AP block in open channels often overlaps that of fast inactivation in many K^+ channels. We have overcome these problems by expressing Kv2.1 and Kv3.1, 4AP-sensitive, slowly-inactivating rat brain K^+ channel clones in *Xenopus* oocytes. This approach has the advantage of sampling either single channels or ensemble averages of many channels from a homogenous population whose density in the surface membrane can be controlled by adjusting by the amount of cRNA injected into the cell.

The present study elucidates 4AP's mechanism and provides a necessary prerequisite to a mutational analysis of the 4AP blocking site in cloned channels. A preliminary report of these results has appeared (Kirsch, Vener, Drewe, and Brown, 1993).

MATERIALS AND METHODS

Recombinant DNA Techniques

Standard methods of plasmid DNA preparation, site-directed mutagenesis and DNA sequencing were used (Sambrook, Fritsch, and Maniatis, 1989; Drewe, Hartmann, and Kirsch, 1993).

Kv2.1 and Kv3.1 were propagated in the transcription-competent vector pBluescript SK(−) in *Escherichia coli* XL1-Blue (Stratagene Corp., La Jolla, CA). A single-stranded DNA template was prepared for specific oligonucleotide-directed mutagenesis by digesting Kv2.1 with *Bam*HI (+909 and +1,520). The resultant 611 nucleotide fragment was subcloned into *Bam*HI-digested M13mp19 single-stranded phagemid. Mutagenesis was performed using an Amersham kit as described previously (Amersham Corp., Arlington Heights, IL) (Kirsch, Drewe, Taglialatela, Joho, DeBiasi, Hartmann, and Brown, 1992*b*). The mutated DNA fragment was cloned back into the original *Bam*HI-cut Kv2.1. The region spanning the BamHI sites was verified by sequencing.

In Vitro Transcription and Oocyte Injection

Stage V or VI oocytes were defolliculated enzymatically (Drewe et al., 1993), injected with 50 nl of cRNA solutions at a concentration of 1–20 pg/nl, and used for recording 1–4 d after injection.

Electrophysiology and Data Analysis

Whole cell currents were recorded in oocytes using a two-intracellular microelectrode voltage clamp as described previously (Drewe et al., 1993). Cell-attached and excised patch recording was performed with oocytes after manual removal of the vitelline envelope, as described previously (Kirsch et al., 1992*a*). Isotonic KCl bathing solution was used to zero the resting potential. Holding and test potentials applied to the membrane patch were reported as conventional absolute intracellular potentials. Experiments were performed at room temperature (21–23°C). Data were low-pass filtered at 0.5–1 kHz. (−3 dB, 4-pole Bessel filter) before digitization at 4 kHz. Channels were activated with rectangular test pulses from negative holding potentials. Holding potentials were adjusted to minimize simultaneous openings of multiple channels. Open and closed transitions were detected using a half-amplitude threshold criterion as described previously (Kirsch et al., 1992*b*).

We used the CSIM program (Axon Instruments, Foster City, California) to simulate single channel and ensemble average currents using a four state model with specific transition rate constants and initial conditions chosen to approximate the experimental data as described in the text.

Data were expressed as means ± SD where appropriate. A two-tailed *t*-test was used to evaluate the significance of the difference between means ($P < 0.05$).

Solutions and Drugs

Bath solution for whole cell recording consisted of (in mM): 50 NaOH, 50 KOH, 100 methanesulfonic acid, 2 $CaCl_2$, 10 HEPES, pH 7.3. Patch pipettes were filled with Na^+ Ringer's solution which consisted of (in mM): 120 NaCl, 2.5 KCl, 2 $CaCl_2$, 10 HEPES, pH 7.3. Depolarizing isotonic KCl bath solution consisted of (in mM): 100 KCl, 10 EGTA, 10 HEPES, pH 7.3. Bathing solution flowed continuously at a rate of 3 ml/min. 4-Aminopyridine (Sigma Chemical Company, St. Louis, Missouri) stock solution was made by dissolving 4AP in bathing solution to a concentration of 20 mM (pH adjusted to 7.3 with HCl). 4-Aminopyridine methiodide (4APMI) was prepared as described previously (Kirsch and Narahashi, 1983).

RESULTS

Differential 4AP Block of Whole Cell Kv2.1 and Kv3.1 Currents

At the whole cell level 4AP produces a much more potent block in Kv3.1 than Kv2.1 channels. Fig. 1 *A* shows superimposed records from a voltage-clamped oocyte that

expressed Kv3.1, obtained before (*c*), after equilibration with drug (0.1 mM 4AP) and after washout with drug-free bathing solution (*w*). During the 15 min 4AP exposure, the cell was stimulated repetitively with 250 ms pulses to +40 mV, delivered at 15-s intervals (records not shown). The 4AP trace shows that ≈60% of the K^+ current was blocked at 0.1 mM. As indicated by trace *w*, block was completely reversed by 45 min exposure to drug-free solution during which the cell was repetitively pulsed (records not shown). In contrast, in oocytes that expressed Kv2.1 (Fig. 1 *B*) a similar level of block required much higher 4AP concentration. The average dose-response relationship obtained by these procedures is shown in Fig. 1 *C*. The smooth curves were fit by a 1:1 binding model with apparent Kd of 0.1 and 17 mM respectively in Kv3.1 (*triangles*) and Kv2.1 (*squares*).

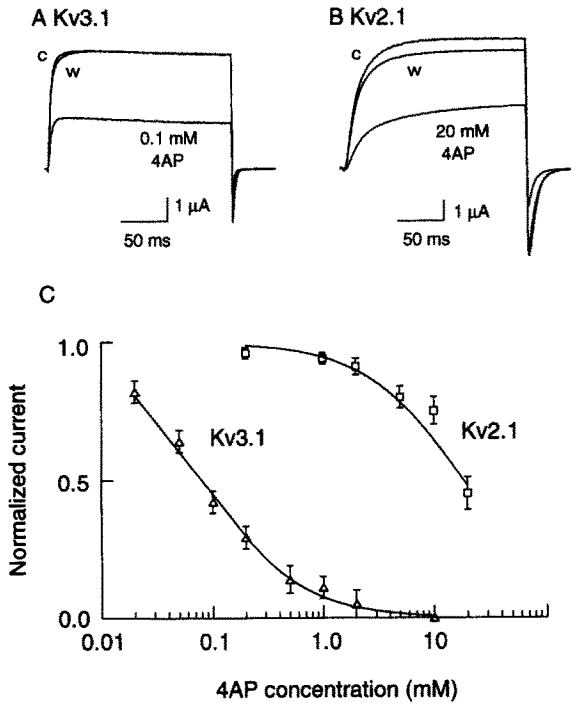

FIGURE 1. Differential 4AP sensitivity in Kv2.1 and Kv3.1. Two-microelectrode voltage clamp records of Kv3.1 (*A*) and Kv2.1 (*B*) channels expressed in *Xenopus* oocytes bathed in low Cl^- solution containing 50 mM $[K^+]_o$ and 50 mM $[Na^+]_o$. Cells were held at −80 mV and stimulated repetitively with 250-ms pulses to +40 mV at 15-s intervals for 250 ms. In *A* and *B*, control traces (*c*), obtained before application of 4AP are superimposed on records obtained after 15 min 4AP equilibration at the concentrations indicated. Reversibility (trace *w*) was determined after 45 min washout with drug-free saline. The cells were pulsed continuously throughout the experiment. *C* shows cumulative dose response data obtained from six cells injected with Kv2.1 (*squares*) and five cells injected with Kv3.1 (*triangles*). Current amplitude at a test potential of +40 mV after drug application was normalized by dividing by control current amplitude obtained before drug application. The data were fit to the equation:

$$\text{Normalized currents} = \text{Kd}/([4\text{AP}]^n + \text{Kd}),$$

where Kd = apparent dissociation constant, [4AP] = 4AP concentration (mM) and n = Hill coefficient.

For Kv2.1 the data were most accurately fit by Kd and n of 17 mM and 1.00, respectively. For Kv3.1 Kd = 0.08 mM and n = 0.95.

Membrane-sidedness of 4AP Block

In the following experiments oocytes were injected with relatively high concentrations (20 pg/nl) of RNA to facilitate measurement of semi-macroscopic currents under patch clamp recording (*macropatch*) conditions. As shown in the *I–V* family in Fig. 2 *A*, the voltage- and time-dependent gating properties of Kv3.1 were similar to those recorded by two-microelectrode whole cell methods. Tail currents were negligibly small in the patch records because the extracellular solution in the pipette contained

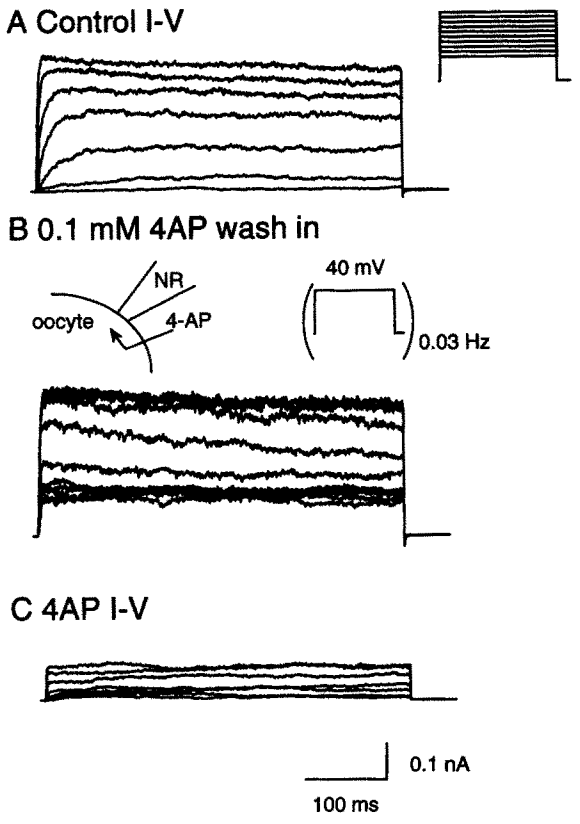

FIGURE 2. Effect of bath-applied 4AP on a cell-attached patch. Semi-macroscopic currents were recorded in a cell-attached patch containing many channels. *A* shows control I-V family of currents evoked by test pulses of −20 to +40 mV (10 mV steps, test pulse protocol shown in the inset). The records were leakage and capacity subtracted by a P/4 protocol. Each trace is signal averaged from four runs. *B* shows the application of 0.1 mM 4AP to the bathing solution (see inset) while monitoring block with repetitive test pulses to +40 mV from holding potential 90 mV at a repetition rate of 0.03 Hz (see inset pulse protocol, no signal averaging or subtraction was done). *C* shows the I-V family (−20 to +40 mV) after 4AP equilibration with averaging and subtraction as in *A*. Extracellular and intracellular solutions were normal Na^+-Ringer's and isotonic KCl, respectively.

only 2.5 mM K^+ compared with 50 mM K^+ in whole cell measurements. In cell-attached patches, application of 0.1 mM 4AP to the bathing solution caused a progressive reduction in outward currents when the patch was repetitively stimulated at 15-s intervals (Fig. 2 *B*) with a constant test pulse potential of +40 mV. A steady-state level of block (Fig. 2 *C*) was reached after 5 min as 4AP diffused across the membrane to accumulate in the intracellular space. In cell-attached patches bath-applied 4AP presumably cannot reach the extracellular side of the patch because of the tight seal formed between the recording pipette and the membrane.

These results suggest that in Kv3.1, as in squid axon (Kirsch and Narahashi, 1983), the 4AP binding site is reached via the cytoplasmic surface of the channel.

Further evidence for an intracellular site was obtained by testing a quaternary 4AP derivative, 4-aminopyridine methiodide (APMI), that cannot readily cross the membrane. Fig. 3 *A* shows the effect of 10 mM 4APMI on an inside-out excised patch. Under control conditions, patch excision causes a progressive acceleration in the rate of inactivation (e.g., compare Fig. 3 *A*, *inset a*, with Fig. 2 *A*) without changing the amplitude of the peak currents. This phenomenon was responsible for the apparent

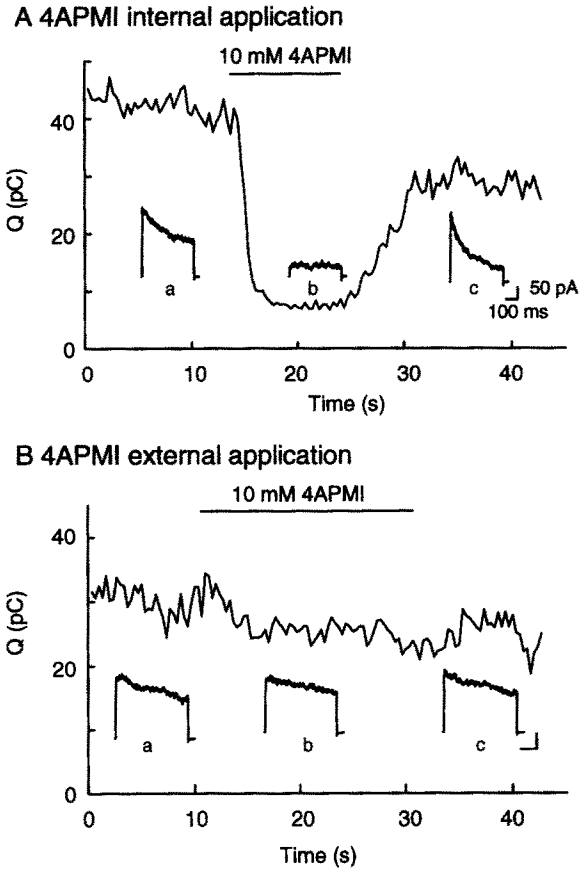

FIGURE 3. Membrane sidedness of 4APMI block. A quaternary 4AP derivative was applied to inside-out (*A*) or outside-out (*B*) patches to determine whether 4AP has access from intra- or extracellular side of the channel. *A* shows a sequence of repetitive pulses to +40 mV from holding potential −90 mV. From the integration of the current records total charge movement was plotted versus time. 10 mM 4APMI was added to the bathing solution as indicated by the horizontal bar. Typical records before (*a*), during (*b*) and after washout of 4APMI (*c*) are shown in the inset. *B* shows the same experiment performed with an outside-out patch. Extracellular solution was Na^+-Ringer's.

"rundown" when comparing control and washout intervals in Fig. 3 *A*, where total charge movement/trace was plotted versus time during repetitive pulsing. Accelerated inactivation can readily be distinguished from 4APMI block by the fast onset of block and its reversibility when the drug was washed from the intracellular surface as shown in Fig. 3 *A*. The effectiveness of 4APMI was abolished when the drug was applied to an outside-out patch as shown in Fig. 3 *B*. Similar results were obtained in three additional inside-out patches and two additional outside-out patches. Thus, in agreement with previous results in squid axon (Kirsch and Narahashi, 1983), 4APMI,

unlike the membrane-permeant parent compound, is effective only when applied internally to Kv3.1.

Gating-dependence of Block in Kv3.1

Recent evidence (Wagoner and Oxford, 1990; Choquet and Korn, 1992) suggests that in some channels, 4AP more readily enters the open than the closed state as judged by experiments in which the level of block achieved during drug application, and the amount of recovery from block during drug wash out, is strongly dependent on channel activation by depolarizing test pulses. A related phenomenon in squid axon may be the acceleration of the rate of block by depolarizing holding potentials (Kirsch et al., 1986). Kv3.1 also shows a pulse-dependent onset and recovery from block (Fig. 4), and more importantly, this effect allows estimation of 4AP ON and OFF rates in the closed channel. An inside-out patch bathed in drug-free solution was pulsed to +40 mV (trace *c*) from a holding potential of −90 mV to measure the control level of current. Stimulation then was suspended while 0.1 mM 4AP was applied to the intracellular surface for a total exposure time of either 15 s (*A*) or 45 s (*C*). During this interval the channels were held in the closed state at −90 mV. Without removing 4AP, repetitive test pulses were resumed starting with trace *1*. As shown in Fig. 4 *A*, before 4AP application (trace *c*) Kv3.1 test pulse current showed a rapid rise to a peak, followed by a slow decay, whereas the first test pulse after 4AP application (trace *1*) evoked a current with reduced peak and faster decay. Subsequent test pulse currents (traces *2–4*, Fig. 4 *A*) showed a steady-state level of block similar to that achieved by continuous pulsing (e.g., Fig. 3). A likely explanation is that 4AP could not readily enter the closed channel, but upon channel activation, the drug equilibrated with a site in the channel. Because, as shown below, drug block of activated Kv3.1 channels proceeds much more slowly than the rate of activation, the reduction of peak current evoked by the first pulse after the exposure interval gives an estimate of the amount of closed channel block during the preceding exposure interval. As shown in Fig. 4 *C* a 30-s increase in the exposure of closed channels gave a markedly increased level of resting channel block as assessed from the peak of trace *1*. A plot of normalized peak current in the first pulse after 4AP application as a function of exposure interval from several patches (Fig. 4 *E*) gave an estimated ON rate of 0.1 s^{-1} mM^{-1}.

Drug trapping in the closed channel was observed upon wash out (Fig. 4, *B* and *D*). The patch was held at −90 mV and the cytoplasmic surface was washed with drug-free solution for 65 s without pulsing. Trace *1* shows that the current evoked by the first pulse after wash out was blocked to the same extent as the currents from channels fully equilibrated with 4AP (Fig. 4, *A* and *C*). Thus, during the wash interval, no drug escaped from the closed channel, but during subsequent pulses (traces *2–4*) we observed a progressive recovery of current as 4AP dissociated from the activated channels. In other experiments we observed no recovery from block in closed channels after washout intervals ≤ 3 min. The dissociation rate from closed channels therefore must be < 0.01 s^{-1}.

Because drug cannot escape from closed channels during the interval between stimuli, the removal of block observed in Fig. 4, *B* and *D*, must take place exclusively from activated channels. Therefore, we have estimated this OFF rate from the

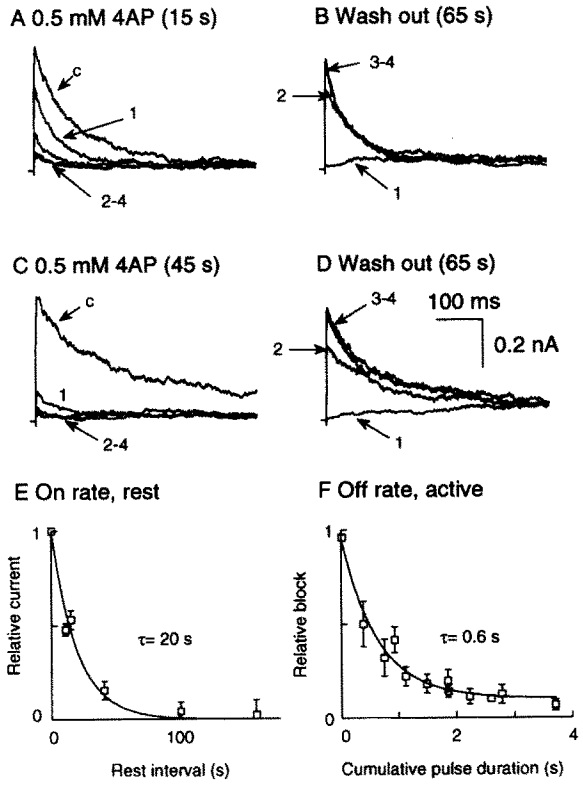

FIGURE 4. Pulse-dependent block and recovery. An inside-out patch was stimulated repetitively at 15 s intervals with 250 ms pulses to +40 mV. In *A*, trace *c* was the last of 16 control pulses, after which stimulation was suspended while 0.1 mM 4AP was applied to the intracellular surface for a total exposure interval of 15 s. The interval represents total time after switching reservoirs minus the time (25 s) required to clear dead space in the superfusion system. Solution exchange rates were measured in each patch by observing block after switching between K^+- and Cs^+-containing solutions. Trace *1* shows the first current evoked upon resumption of stimulation during maintained exposure to 4AP. Traces *2–4* show subsequent currents evoked by repetitive stimulation at 15 s intervals. *B* shows a wash out experiment in which pulsing was suspended while the intracellular surface was washed with drug-free saline for a total exposure interval of 65 s. Traces *1–4* show the currents evoked upon resumption of repetitive stimulation in the continued absence of drug. *C* and *D* repeat the experiment in the same patch but with 45 s 4AP exposure interval. Please note that experiments *C–D* were performed before *A–B*. Therefore, the different decay rates of currents in the control (*c*) traces in (*A*) and (*C*) actually shows the progressive acceleration of the rate of inactivation that occurs spontaneously in inside-out patches containing Kv3.1. *E* shows the time course of block in pooled data from nine patches obtained by the interrupted pulse protocol described above. Peak currents from the first trace upon resumption of stimulation were normalized to control currents and plotted versus exposure interval to obtain the time constant for the onset of block in resting channels as described in the text. *F* shows the rate of removal of block from activated channels in wash out experiments (e.g., *B–D*). Isochronal currents (10 ms from the beginning of the test pulse) were normalized to the maximum current after complete wash out. Relative block = 1-relative current. Drug does not escape from closed channels during the 15-s interval between pulses, the abscissa therefore, plots time as cumulative pulse duration of successive stimuli.

progressive increase in peak currents during the wash out as shown in Fig. 4 *F*. The time base is cumulative test pulse duration during repetitive stimulation. The smooth curve shows a biexponential fit of the data with fast τ = 0.6 s and a much slower τ = 7 s. We believe the fast time constant which accounts for 90% of the decay represents 4AP OFF rate from channels in an unrestricted diffusion space. The small, slow

component of wash out also was observed in control experiments (data not shown) in which Cs^+ and K^+ were exchanged at the cytoplasmic surface and may reflect diffusion delays associated with patch geometry.

A Kinetic Model of 4AP Block in Kv3.1

From the preceding results, channel activation appears to control 4AP access to a binding site in the channel. Once inside the channel, however, 4AP is trapped by the closing of the activation gate such that recovery from block cannot proceed until the channel reopens. Fig. 5, *A–B*, shows a simple kinetic scheme and simulated current records that provide a framework for these and later results. We assume that the channel has multiple closed states, that for simplicity are combined into a single

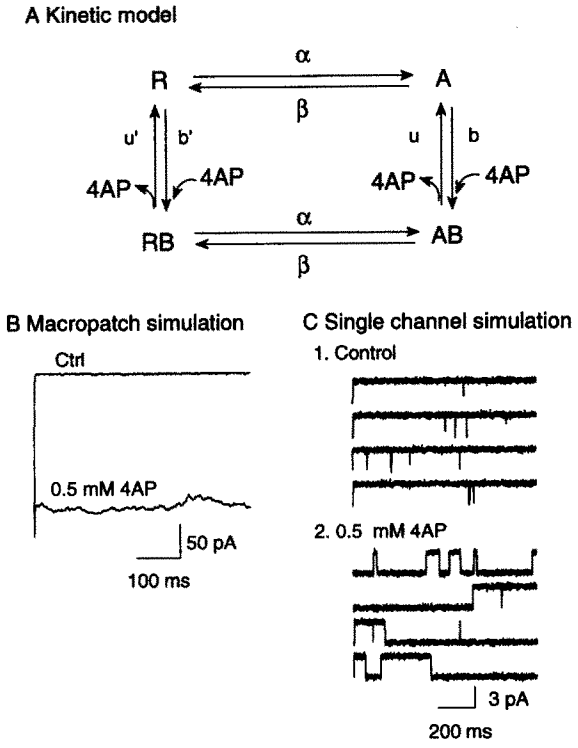

FIGURE 5. A kinetic model for 4AP block in Kv3.1. Channel gating is simplified in this model by combining several closed states into one resting *R* state that is occupied at negative potentials. The activated, ion conducting state *A*, that is populated at depolarized potentials, combines the open state and proximal closed states observed during bursting. Gating transitions between *R* and *A* proceed via voltage-dependent rates α and β. 4AP can bind reversibly to either *R* and *A* to form *RB* and *AB*, respectively. Gating transitions between the latter are assumed to proceed normally, but *AB* is nonconducting. Rate constants, u' and b', respectively are unblock (*OFF*) and block (*ON*) rates for resting channel block. Estimates of u' and b', from experiments described in the preceding figure, were 0.01 s^{-1} and 0.1 s^{-1} mM^{-1}, respectively. OFF and ON rates in activated channels are denoted u and b, respectively. Estimates of u and b, from single channel experiments were 2.4 s^{-1} and 21 s^{-1} mM^{-1}, respectively. *B* and *C* show simulated current records in the presence and absence of 0.5 mM 4AP, obtained by setting α and β, to 1,000 and 2.5 s^{-1}, respectively, to approximate gating at a test potential of +40 mV. Initial conditions were set to simulate 4AP trapping in closed channels at a holding potential of −90 mV, after steady state equilibration with activated channels (i.e., simulation of experiments of Fig. 2 and 6, respectively, in *B* and *C*). *B* simulates a macropatch containing 80 channels. Each trace is the average of four simulation runs. *C* simulates a patch containing a single channel.

resting state (*R*). Also because of limited frequency response of the recording system we can detect only bursts of openings from activated channels. Thus, the activated state (*A*) combines the open state and brief closed states associated with bursting. At the holding potential, channels in the resting state are available for voltage-dependent activation that proceeds via rate constants α and β. As shown below, these simplifications are reasonable for Kv3.1 stimulated by a test potential of +40 mV, because average waiting time for activation (i.e., latency from the beginning of the test pulse to the first opening in the record) was complete within 10 ms and was much faster than drug block rates. 4AP can enter resting channels (*RB*) with ON rate constant, b′ (0.1 s^{-1} mM^{-1} from macropatch experiments, Fig. 4 *E*). RB channels will gate normally upon stimulation to reach an activated-blocked state (*AB*). Although the OFF rate from closed channels, u′, was too slow to measure directly, macropatch experiments (Fig. 4, *B–D*) set 0.01 s^{-1} as an upper limit. The scheme also provides a direct pathway for 4AP interaction with activated channels. The rate constants for block (*b*) and unblock (*u*) can be estimated from single channel kinetics or, in the case of unblock, from the macropatch wash out experiment (Fig. 4 *F*).

As shown in Fig. 5 *B*, substitution of experimentally determined rate constants (see below) adequately simulates the waveform of macropatch currents after full equilibration of 4AP in activated channels. Notably, the simulated 4AP-blocked currents, like the real currents, show little time-dependent change in the amount of block during a long test pulse, despite the fact that 4AP caused long delays in first latencies in the simulated single channel currents (Fig. 5 *C2*). The characteristic features of 4AP block in single channels are examined in the following sections.

4AP Block in Single Kv3.1 Channels

Although peak Kv3.1 currents resist rundown in excised patches, the progressive increase in the apparent rate of inactivation (i.e., decay of current during a test pulse) complicates the estimation of the 4AP ON and OFF rates in the activated channel. In this section block rates were estimated from single channel records in cell-attached patches that show stationary gating kinetics.

Oocytes were injected with dilute RNA solution (1 pg/nl) to reduce the number of channels in membrane patches. Six patches that contained only a single active channel (as judged by the absence of overlapping openings of multiple channels when the patch was repetitively stimulated 128 times at 0.3 Hz with pulses designed to achieve maximum activation in control records) were selected for detailed analysis. Records were obtained in each patch before and after equilibration with bath-applied 4AP. A typical example of control records is shown in Fig. 6 *A* where test pulses of +40 mV amplitude and 925 ms duration evoked channel openings almost immediately upon depolarization. The channel remained open in bursts that lasted as long as the patch remained depolarized (trace length coincided with test pulse duration). Thus, the probability of opening versus pulse number (Fig. 6 *C*) was nearly 1.0 in control records. The few gaps are null traces in which the channel was inactivated at rest. In contrast, after 4AP (Fig. 6 *D*) the diary of P_0 versus pulse number showed many more gaps that are related to drug block in resting channels rather than inactivation for reasons discussed below. 4AP also caused an overall reduction in open time/trace, consistent with long blocked periods during the test pulse.

After equilibration with 4AP, the pattern of openings in individual traces showed two distinctive new features (Fig. 6 *B*) when compared with control records: shortened burst duration and prolonged first latencies. After 4AP, a mean burst duration of 50 ms was estimated from the time constant obtained by fitting the burst duration histogram (Fig. 7 *B*) to a monoexponential decay and, as shown in Fig. 7 *C*, (burst length)$^{-1}$ increased with 4AP concentration. The control histogram (Fig. 7 *A*), in contrast, showed an average time constant of 400 ms (n = 6). Thus, as indicated in the kinetic scheme of Fig. 5, dwell time in the activated state at a test potential of +40 mV was ~0.4 s, corresponding to β = 2.5 s^{-1}. This calculation, however, can be taken only as an upper limit since estimated burst length did not include bursts that

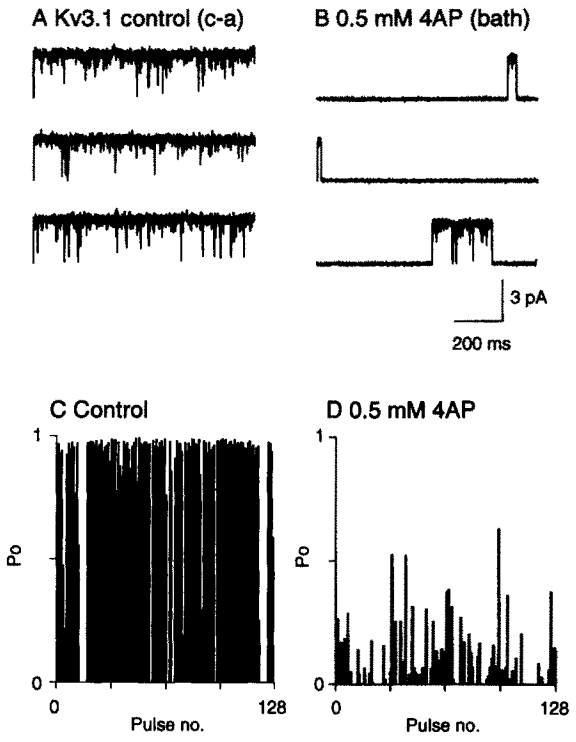

FIGURE 6. 4AP block in single Kv3.1 channels. *A* shows control records obtained in a cell-attached, single channel patch pulsed repetitively to +40 mV from a holding potential of −90 mV for 925 ms. The length of the trace is coincident with the duration of the pulse. *B* shows records obtained 15 min after addition of 0.5 mM 4AP to the bathing solution. Extracellular and intracellular solutions were normal Na^+-Ringer's and isotonic KCl, respectively. *C* (*control*) and *D* (4AP) show diaries of probability of opening/trace versus pulse number.

were cut short by repolarization at the end of the test pulse. Nonetheless, 4AP at 0.1 mM, corresponding to the macroscopic IC_{50}, shortened burst length by 60%. The additional decrement at higher drug concentration (Fig. 7 *C*) is consistent with block of the activated channel with ON rate, 21 s^{-1} mM^{-1}.

As indicated by the sample records in Fig. 6 *B* and quantitated in Fig. 8, first latency was markedly prolonged by 4AP (e.g., the first and last traces in Fig. 6 *B*). Brief latencies such as that shown in the middle trace, were more frequent at lower 4AP concentration. Fig. 8, *A–B*, compares the first latency distributions (abscissa is plotted on a logarithmic scale) in control (*A*) and after 4AP application (*B*). The smooth curves show the fit of the data to sums of exponential decays. Control first

latency distributions showed a single peak corresponding to a monoexponential decay with average time constant 1.2 ± 1.0 ms (n = 6). Thus, in the kinetic scheme of Fig. 5, at a test potential of +40 mV, the dwell time in the resting state is ~1 ms, corresponding to α = 1,000 s^{-1}. After 0.5 mM 4AP application (Fig. 8 *B*) the first latency histogram showed an additional peak with average time constant 530 ± 154 ms (n = 4), that corresponds to the long, drug-induced latencies seen in the current traces (Fig. 6 *B*). At a concentration 0.1 mM (≈IC_{50}), 4AP increased first latency by a factor of 440 fold (n = 2).

Long first latencies in the presence of 4AP may have several possible causes: (*a*) 4AP might stabilize the closed state resulting in a shift of the voltage dependence of

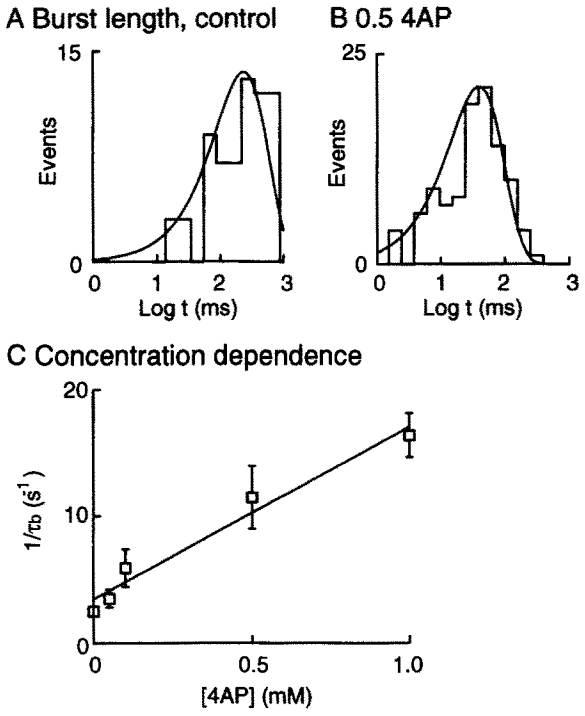

FIGURE 7. Effect of 4AP on burst length. *A* (*control*) and *B* (4AP) show burst length histograms plotted logarithmically (five bins/decade). Bursts were defined by a critical closed interval of 5 ms. Data obtained at a test potential of +40 mV. The smooth curves show monoexponential fits of the data with time constants of 300 and 50 ms in control and 4AP, respectively. *C* shows the 4AP concentration dependence of burst duration (at +40 mV) in pooled data (mean ± SD, n ≥ 3 patches/point), plotted as the reciprocal of the burst duration time constant (s^{-1}) versus 4AP concentration (mM). The straight line is a linear regression fit to the data.

activation to more positive potentials. We have recently reported however, that in Kv3.1 4AP shifts activation −5 mV, an amount consistent with reduced series resistance error (Kirsch et al., 1993). (*b*) 4AP might interfere with gating such that drug-bound channels activate slowly. This explanation also seems unlikely in view of the results of Spires and Begenisich (1989) who showed that K^+ channel gating currents in squid axon were unaffected by 4AP at concentrations sufficient to block ionic current. (*c*) Long first latencies are the result of the slow time course of 4AP dissociation from open channels that activate normally even when occupied by 4AP. Thus, according to the kinetic scheme (Fig. 5), this slow component represents dwell time in state AB. Our observations provide support for this notion. First, the time constant of the slow component of the first latency distribution was similar to the time

constant for wash out of 4AP from the activated channels (Fig. 4, *B, D, F*) in excised patches. Second, the time constant of the slow component at a test potential of +40 mV was not significantly different from that obtained at 0 mV (average $\tau = 450 \pm 70$ ms, $n = 4$). This would be expected only if voltage-independent 4AP dissociation rather than a voltage-dependent step in channel gating were rate-limiting. Thus, the slow component of the first latency distribution yields a rate constant, u = 2.4 s^{-1}, that represents 4AP dissociation from the activated state (Fig. 5).

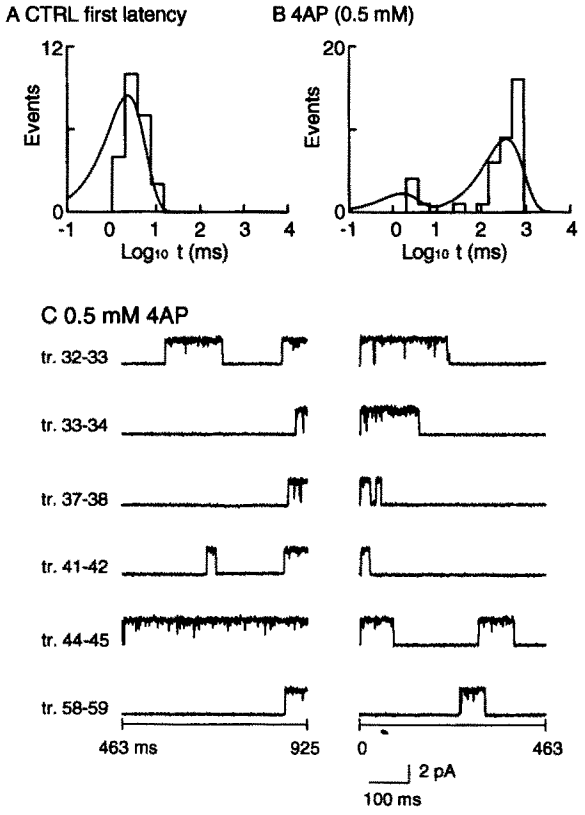

FIGURE 8. Effect of 4AP on first latency. *A* (*control*) shows a histogram of first latency (waiting time from the beginning of the test pulse to the first opening in the record, plotted logarithmically) obtained in a cell-attached, single channel patch at test potential +40 mV. The data are fit by a monoexponential function with time constant of 2 ms. *B* shows a logarithmic plot of first latencies in the same cell-attached, single channel patch obtained from 64 test pulses (amplitude +40 mV, holding potential −90 mV, pulse duration 925 ms, pulse interval 2 s). The fast and slow time constants (and areas) were 2 (0.2) and 492 ms (0.8), respectively. *B* shows consecutive pairs of traces (left-hand and right-hand columns, respectively, show last half and first half of the paired traces) in which the first record of the pair ends with an unblocked channel opening. In 5/6 pairs an unblocked channel opening at the end of the first trace was coupled with a short first latency in the next trace, thus demonstrating the slow rate of 4AP entry into the closed channel during the 2-s interval between pulses.

The fast component that appears in the 4AP first latency histogram (Fig. 8 *B*) resembled that obtained in control. We suggest, therefore, that the short waiting times arise when the channel is unoccupied by 4AP in the closed interval before the test pulse, and that the long waiting times occur when 4AP is trapped within the channel and dissociates slowly (compared to gating) from the activated channel. If 4AP can be trapped in the closed channel we would expect that traces with long first latencies would show a previous history of being blocked by 4AP. Similarly, if 4AP can be prevented from entering a closed, unblocked channel we would expect traces with

short first latencies to show evidence of being unoccupied by 4AP at the end of the preceding trace. The latter effect is shown in Fig. 8 *C* where the channel was pulsed repetitively (64 pulses) to +40 mV from a holding potential of −90 mV at 0.3 Hz after 4AP equilibration. The waiting time distribution was bimodal (Fig. 8 *B*) with time constants of 2 and 492 ms that presumably represent normal and 4AP-occupied conditions, respectively. From this sample of 64 traces we selected all of the records (left half of Fig. 8 *C*) which ended with an unblocked channel, i.e., an open event cut short by repolarization at the end of the test pulse. We then examined the first latencies of the next trace in sequence for each record as shown in Fig. 8 *C* (*right*). Remarkably, in the first five pairs of traces, channels that were unblocked at the end of the first pulse showed normal first latencies at the beginning of the next trace. These five records account for the 2-ms peak in the first latency histogram (Fig. 8 *B*). Thus, in this experiment, all of the short first latencies are correlated with unblocked channels. A close correlation of long latency with a previously blocked channel also was obtained with the exception of the paired traces *58–59*. In this case, an unblocked channel became blocked during the rest interval, consistent with the observation in Fig. 4, *A* and *B*, that 4AP has access to resting channels albeit at a slow rate. We pooled data from 918 traces in four single channel patches treated with 0.5 mM 4AP to obtain a better estimate of the correlation of unblocked channels with short latencies, and blocked channels with long latencies. We used the criteria that a blocked interval at the end of a pulse must be >31 ms, i.e., three times the control interburst interval, and an unblocked interval at the beginning of a pulse must be <5 ms, i.e., three times the mean first latency. In the expanded data set the probability of an unblocked channel having long latency (presumably by becoming blocked during the rest interval) was <0.3 and the probability of a blocked channel having short latency (presumably by becoming unblocked during the rest interval) was <0.04. Although there is some uncertainty in distinguishing between blocked, closed and inactivated states, these results indicate that 4AP has a low probability of entering the closed channel and is virtually prevented from leaving during the two second resting interval between pulses. Furthermore, the long first latencies introduced by 4AP reflect the rate of drug dissociation from activated channels.

Gating-dependence of 4AP Block in Kv2.1

The difference in 4AP sensitivity between Kv2.1 and Kv3.1 might be taken to indicate two blocking sites with different affinities. However, the observations described in this section suggest that the mechanism, and therefore the binding site, is the same in both channels. Kv2.1 is less suitable for detailed single channel measurement because of its low conductance compared with Kv3.1 (Hartmann et al., 1991) and its susceptibility to rapid rundown after patch excision (unpublished observations). Also, because gating and drug block take place on roughly the same time scale, quantitative estimation of block rates from single channel data was not possible. However, bath application of 4AP at 20 mM to a cell-attach patch containing a single channel (Fig. 9) shows that 4AP blocks Kv2.1 via a cytoplasmic pathway and evokes a qualitatively similar pattern to that observed in Kv3.1. Thus, 4AP reduced the level of channel activity (Fig. 9 *D*) by a decrease in burst duration and an increase in first latency (Fig. 9 *B*). Kinetic analysis in four single channel patches showed that 4AP at

a concentration $\approx IC_{50}$ caused a 60% reduction in burst duration and eightfold increase in first latency, compared with 60% and 440-fold respectively in Kv3.1 at the IC_{50} concentration of 4AP. It should be noted that an equal reduction in burst duration required 200 times more 4AP in Kv2.1 than in Kv3.1. Because kinetic changes are related to 4AP ON and OFF rates in the activated channel, we suggest that Kv2.1's low sensitivity to 4AP may be caused by both decreased association and increased dissociation rates.

4AP block in Kv2.1, as in Kv3.1 was strongly accelerated by channel activation. This phenomenon was observed qualitatively at the whole cell level (Fig. 10) in an

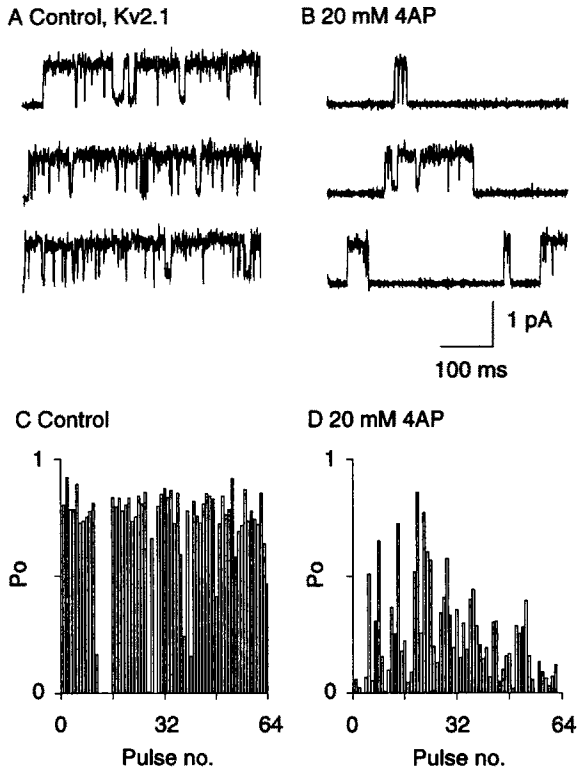

FIGURE 9. 4AP block in single Kv2.1 channels. *A* shows control records obtained in a cell-attached, single channel patch pulsed repetitively to +60 mV from a holding potential of −80 mV for 463 ms. The length of the trace is coincident with the duration of the pulse. *B* shows records obtained 11 min after addition of 20 mM 4AP to the bathing solution. Extracellular and intracellular solutions were normal Na^+-Ringer's and isotonic KCl, respectively. *C* (*control*) and *D* (4AP) show diaries of probability of opening/trace versus pulse number.

interrupted pulse experiment similar to that of Fig. 4. The test was performed in both the wild type channel and a mutant channel (Kv2.1 T368V + I369V) in which the voltage dependence of activation was shifted 20 mV in the depolarizing direction. As shown in Fig. $10A_2$, the first pulse (trace *1*) after a prolonged exposure to 5 mM 4AP during which the cell was clamped at −80 mV, shows less block than subsequent pulses (traces *2–6*), consistent with restricted access to the blocking site in the closed channel. After 4AP wash out the experiment was repeated with the cell held at −40 mV during the same duration of 4AP exposure. In this case (Fig. $10\ A_1$) however, the pattern of current traces was markedly different; the first pulse upon resumption of stimulation (trace *1*) showed a greater degree of block than subsequent pulses. This result suggests that a holding potential of −40 mV facilitates 4AP access to the

blocking site and that the affinity of the channel for 4AP is greater at −40 mV than at the test potential of +40 mV. This might be the case if the blocking rate constants depend on activation gating, such that at −40 mV the channels are partially activated. This idea was tested by repeating the measurement in a mutant channel in which the voltage dependence of activation was shifted by +20 mV (Fig. 10 *C*). As

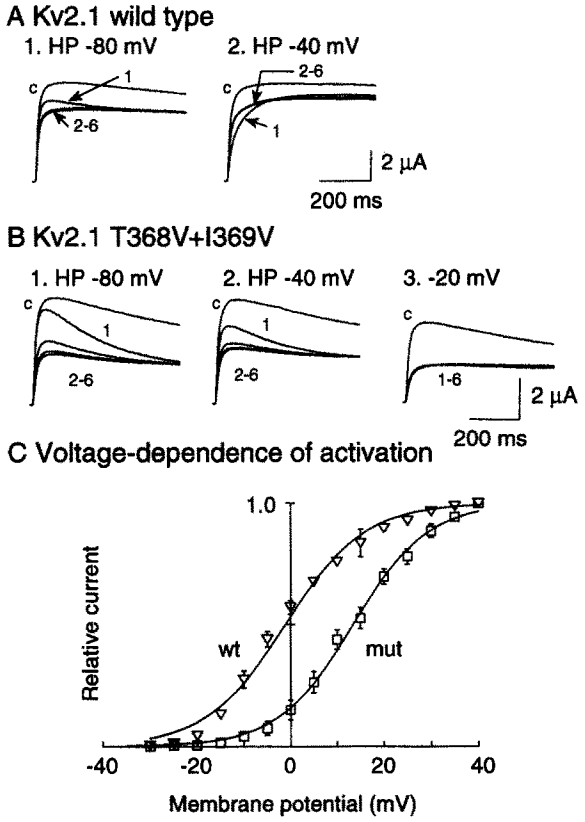

FIGURE 10. Holding potential dependence of 4AP block in Kv2.1. *A1* shows superimposed Kv2.1 whole cell currents evoked by test pulses to +40 mV from the holding potential indicated. Trace *c* was recorded before 4AP application. Stimulation was suspended and the cell was exposed to 5 mM 4AP for 5 min. Repetitive stimulation (15-s interval) was resumed (traces *1–6*). Note that block did not reach steady state until trace *2*. *A2* shows the same experiment performed at a holding potential of −40 mV, in the same cell after 4AP washout. Note that the amount of block at the beginning of trace *1* was greater than in subsequent traces, indicating block accumulation during the exposure interval at the holding potential of −40 mV. *B1–3* shows a similar interrupted pulse experiment in another cell that expressed a mutant Kv2.1 channel in which two residues in the P-region (Hartmann et al., 1991) were changed. As shown in *C*, the voltage dependence of activation in the mutant channels (*squares*) compared with wild type (*triangles*) was shifted 14.2 mV in the depolarizing direction. The data were obtained from whole cell chord conductance measurements at test potentials of −30 to +40 mV (5 mV increments). Conductances were normalized to the maximum at +40 mV. Mean ± SE (n = 5 and 4, respectively for wild type and mutant channels) data are plotted versus test pulse potential. Smooth curves show Boltzmann fits to the data.

shown in Fig. 10 *B*, the holding potential required to shift the pattern of 4AP block to that observed in wild type at −40 mV also was shifted by roughly 20 mV (compare A_2 and B_3) in the mutant. We suggest therefore, that the 4AP mechanism is qualitatively the same in both Kv2.1 and Kv3.1 channels, but mutations that affect gating may also influence 4AP block.

DISCUSSION

In this study we have exploited the advantages of the oocyte expression system to compare 4AP block in Kv2.1 and Kv3.1, two voltage-gated K^+ channels that also are the subjects of extensive mutational analysis (Hartmann et al., 1991; Kirsch et al., 1992*a*). We found that the two channels differ markedly in their sensitivity to 4AP, but the mechanism of action in both was qualitatively similar. Therefore, the quantitative differences in block may be specified by amino acid substitutions in the same region of both channels. Two critical regions in transmembrane segments S5 and S6 have recently been identified by mutational analysis (Kirsch, Shieh, Drewe, Vener, and Brown, 1993).

Differential 4AP Sensitivity of Kv3.1 and Kv2.1

The high sensitivity of Kv3.1 reported here compares well with that reported in the original characterization of the clone (Yokoyama, Imoto, Kawamura, Higashida, Iwabe, Miyata, and Numa, 1989). But the low sensitivity of Kv2.1 is markedly different from that originally reported (Frech, VanDongen, Schuster, Brown, and Joho, 1989). Because no details were given in the latter report, we suspect that differences in experimental factors, such as external pH and test pulse potential, might be responsible for the discrepancy. Our results agree more closely with those of Pak, Covarrubias, Ratcliffe, and Salkoff (1991), who showed that m*Shab*, a channel that shares complete sequence identity with Kv2.1 in the membrane-spanning core of the protein, was insensitive to 4AP at concentrations to 5 mM.

Gating-dependent 4AP Mechanism in Kv3.1 and Kv2.1

Previous studies in a variety of cells have provided support for the idea that 4AP selectively blocks either closed channels (Yeh et al., 1976; Kehl, 1990) or open channels (Århem and Johansson, 1989; Wagoner and Oxford, 1990; Choquet and Korn, 1992). The interpretation of these results, however, suffers from heterogeneity of K^+ channel subtypes in native cells. Our study measured the effect of gating on 4AP rates and provides clear evidence that in a homogeneous channel population, 4AP can bind to both open and closed conformations. Also we show that 4AP can be trapped in the closed channel and that this effect can account for the long first latencies observed previously in single channel recordings (Choquet and Korn, 1992).

Kv3.1 was particularly well suited for in depth analysis of 4AP block because of its relatively high single channel conductance, resistance to rundown in excised patches and fast activation kinetics relative to 4AP rates. Our single channel and macropatch experiments showed that 4AP is trapped in closed channels for periods of several minutes, but can be released from activated channels in a fraction of a second. Similarly, 4AP access to closed channels is slow. Entry takes place over a period of many seconds, whereas block of activated channels is complete within a fraction of a second. Based on these results, we have proposed a kinetic model (Fig. 5 *A*) in which 4AP block in closed channels takes place with rate constants about 200 times slower than in activated channels. This model and the underlying observations are similar to those obtained in squid axon K^+ channels (Yeh et al., 1976). In squid, 4AP interacts with both the closed and open states but with different rates. Block proceeds in the

closed channel with time constants of 3–30 s compared with 10–25 ms in the open channel. As in Kv3.1, 4AP can enter but not leave closed squid channels. These channels differ quantitatively from Kv3.1 in equilibrium block of the activated channel. In squid, kinetic analysis gave an apparent Kd of 4 mM (Yeh et al., 1976) compared with 0.1 mM in Kv3.1. However, differences in experimental conditions such as temperature and ionic strength may also play a role. Both in squid axon macroscopic currents (Kirsch et al., 1986) and in Kv3.1 we do not know whether channel activation must actually reach the open state before the gating-dependent acceleration of 4AP block occurs. Because our measurements of burst duration include both open time and brief intra-burst closed intervals in Kv3.1, these data also are consistent with the notion that block rates are accelerated after partial activation. This explanation has been offered previously (Kirsch et al., 1986) to account for the observation that in squid axon, the voltage threshold for block acceleration matched the apparent threshold for channel activation.

Although we have less complete measurements in Kv2.1, this channel shows many of the same features as Kv3.1, including restricted entry to and exit from closed channels, intracellular route of access to the binding site, and qualitatively similar pattern of 4AP effects on single channels. The larger effect of 4AP in prolonging first latencies in Kv3.1 compared with the effect in Kv2.1 suggest that high 4AP sensitivity in the former channel was achieved in part by its slow dissociation rate from the activated channel. Because we were unable to distinguish irreversible rundown in excised Kv2.1 patches from 4AP block, we could not determine directly whether drug dissociation from closed channels also was faster in Kv2.1 compared with Kv3.1. But the changes in block during repetitive stimulation (e.g., Fig. 10) compared with total steady state block of activated Kv2.1 channels suggests that equilibration of drug with the closed state may be faster in Kv2.1 than Kv3.1 where frequency-dependent block was not observed. The observation that both Kv2.1 and squid axon channels (Yeh et al., 1976; Kirsch et al., 1986) have low 4AP affinity and frequency-dependent relief of block in the activated state suggests that the structure of the binding sites of the two channels may be related. This result is consistent with the preliminary finding that squid axon K^+ currents show immunoreactivity to a Kv2.1-specific antibody (Caputo, Trimmer, and Bezanilla, 1992).

Site of Action

Our conclusion that 4AP enters the channel via a cytoplasmic route is based on the observations that in both Kv3.1 and Kv2.1, bath application of drug to cell attached patches was very effective, although slow in onset. This would not be the case if exposure of the extracellular surface of the channel were necessary for block. Furthermore, in Kv3.1 we showed that a permanently charged 4AP analog was effective only when applied to the intracellular surface. This result, together with the observed high accessibility of the activated versus the closed channels, suggests that the 4AP site is within the aqueous lumen of the open channel. Previous investigators (Wagoner and Oxford, 1990) were unable to detect a voltage dependence of block independent of the voltage-dependence of gating. We have made similar observations in Kv3.1 (Kirsch et al., 1993) in whole cell voltage clamp. This indicates that the

4AP site unlike that of TEA (Armstrong, 1971; Taglialatela, VanDongen, Drewe, Joho, Brown, and Kirsch, 1991) may be located outside the membrane electric field.

Our results indicate that differences in 4AP interaction between K^+ channel subtypes primarily reflect changes in affinity of 4AP for the activated channel. Furthermore, the exquisite sensitivity of 4AP block rates to activation suggests that the drug site may be closely associated with a cytoplasmic region of the pore that couples the voltage sensor to the ion conduction pathway. Our observation that 4AP can be trapped in channels for periods of several minutes indicates that 4AP is a useful probe of the inner mouth of K^+ pores.

We thank Dr. A. M. Brown for his support and encouragement. We thank G. Schuster and W.-C. Dong for expert oocyte injection and culture; M. Champagne, S. Zhang, and M. Lindsey for molecular biology assistance, and D. George for secretarial assistance.

This work was supported in part by National Institutes of Health grant NS29473 (G. E. Kirsch) and a grant-in-aid from the American Heart Association, Texas Affiliate (J. A. Drewe).

Original version received 12 April 1993 and accepted version received 9 July 1993.

REFERENCES

Århem, P., and S. Johansson. 1989. A model for the fast 4-aminopyridine effects on amphibian myelinated nerve fibres. A study based on voltage-clamp experiments. *Acta Physiologica Scandinavica.* 137:53–61.

Armstrong, C. M. 1971. Interaction of tetraethylammonium ion derivatives with the potassium channels of giant axons. *Journal of General Physiology.* 58:413–437.

Caputo, C., J. S. Trimmer, and F. Bezanilla. 1992. An antibody against the DRK1 K channel affects K currents in squid. *Biophysical Journal.* 61:A376. (Abstr.)

Choquet, D., and H. Korn. 1992. Mechanism of 4-aminopyridine action on voltage-gated potassium channels in lymphocytes. *Journal of General Physiology.* 99:217–240.

Drewe, J. A., H. A. Hartmann, and G. E. Kirsch. 1993. K^+ channels in mammalian brain: a molecular approach. *Methods in Neuroscience.* In press.

Frech, G. C., A. M. J. VanDongen, G. Schuster, A. M. Brown, R. H. Joho. 1989. A novel potassium channel with delayed rectifier properties isolated from rat brain by expression cloning. *Nature.* 340:642–645.

Hartmann, H. A., G. E. Kirsch, J. A. Drewe, M. Taglialatela, R. H. Joho, and A. M. Brown. 1991. Exchange of conduction pathways between two related K^+ channels. *Science.* 251:942–944.

Kehl, S. J. 1990. 4-Aminopyridine causes a voltage-dependent block of the transient outward K^+ current in rat melanotrophs. *Journal of Physiology.* 431:515–528.

Kirsch, G. E., and T. Narahashi. 1983. Site of action and active form of aminopyridines in squid axon membranes. *Journal of Pharmacology and Experimental Therapeutics.* 226:174–179.

Kirsch, G. E., D. F. Vener, J. A. Drewe, and A. M. Brown. 1993. Modulation of 4-aminopyridine block by mutation of deep pore residues in delayed rectifier K^+ channels. *Biophysical Journal.* 64:A226. (Abstr.)

Kirsch, G. E., J. Z. Yeh, and G. S. Oxford. 1986. Modulation of aminopyridine block of potassium currents in squid axon. *Biophysical Journal.* 50:637–644.

Kirsch, G. E., J. A. Drewe, H. A. Hartmann, M. Taglialatela, M. de Biasi, A. M. Brown, and R. H. Joho. 1992*a*. Differences between the deep pores of K^+ channels determined by an interacting pair of nonpolar amino acids. *Neuron.* 8:499–505.

Kirsch, G. E., J. A. Drewe, M. Taglialatela, R. H. Joho, M. De Biasi, H. A. Hartmann, and A. M. Brown. 1992*b*. A single nonpolar residue in the deep pore of related K^+ channels acts as a K^+:Rb^+ conductance switch. *Biophysical Journal.* 62:136–144.

Kirsch, G. E., C-C. Shieh, J. A. Drewe, D. F. Vener, and A. M. Brown. 1993. Segmental exchanges define 4-aminopyridine binding and the inner mouth of K^+ pores. *Neuron.* In press.

Kirsch, G. E., M. Taglialatela, and A. M. Brown. 1991. Internal and external TEA block in single cloned K^+ channels. *American Journal of Physiology.* 261:C583–C590.

Pak, M. D., M. Covarrubias, A. Ratcliffe, and L. Salkoff. 1991. A mouse brain homologue of the *Drosophila Shab* K^+ channel with conserved delayed-rectifier properties. *Journal of Neuroscience.* 11:869–880.

Sambrook, J., E. F. Fritsch, and T. Maniatis. 1989. Molecular Cloning: A Laboratory Manual. Cold Spring Harbor Laboratory, Cold Spring Harbor, New York.

Spires, S., and T. Begenisich. 1989. Pharmacological and kinetic analysis of K channel gating currents. *Journal of General Physiology.* 93:263–283.

Taglialatela, M., A. M. J. VanDongen, J. A. Drewe, R. H. Joho, A. M. Brown, and G. E. Kirsch. 1991. Patterns of internal and external tetraethylammonium block in four homologous K^+ channels. *Molecular Pharmacology.* 40:299–307.

Thompson, S. 1982. Aminopyridine block of transient potassium current. *Journal of General Physiology.* 80:1–18.

Ulbricht, W., and H.-H. Wagner. 1976. Block of potassium channels of the nodal membrane by 4-aminopyridine and its partial removal on depolarization. *Pflügers Archiv.* 367:77–87.

Wagoner, P. K., and G. S. Oxford. 1990. Aminopyridines block an inactivating potassium current having slow recovery kinetics. *Biophysical Journal.* 58:1481–1489.

Yeh, J. Z., G. S. Oxford, C. H. Wu, and T. Narahashi. 1976. Dynamics of aminopyridine block of potassium channels in squid axon membrane. *Journal of General Physiology.* 68:519–535.

Yellen, G., M. Jurman, T. Abramson, and R. MacKinnon. 1991. Mutations affecting internal TEA blockade identify the probable pore-forming region of a K^+ channel. *Science.* 251:939–942.

Yokoyama, S. K., T. Imoto, T. Kawamura, H. Higashida, N. Iwabe, T. Miyata, and S. Numa. 1989. Potassium channels from NG-108-15 neuroblastoma-glioma hybrid cells: primary structure and functional expression from cDNAs. *FEBS Letters.* 259:37–42.